

Effect of Impurity Impact Ionization on the Dynamic Characteristics of 4H-SiC $p^+ - n^- - n^+$ Diodes at Low Temperatures (77 K)

P. A. Ivanov*, A. S. Potapov, and T. P. Samsonova

Ioffe Physical–Technical Institute, Russian Academy of Sciences, ul. Politekhnicheskaya 26, St. Petersburg, 194021 Russia

*e-mail: Pavel.Ivanov@mail.ioffe.ru

Submitted November 18, 2014; accepted for publication November 25, 2014

Abstract—The low temperature (77 K) transient switch-on characteristics of 4H-SiC $p^+ - n^- - n^+$ diodes are measured in the pulse mode. Using a simple analytical model, the effect of impurity breakdown in a heavily doped p^+ -type emitter on the current rise dynamics after applying high-amplitude forward-bias pulses to the diode is explained.

DOI: 10.1134/S1063782615070118

1. INTRODUCTION

Until recently, no attention was paid to the electrical properties of silicon carbide $p-i-n$ diodes at low temperatures. The lack of such interest is mainly associated with the fact that free carriers in SiC are rapidly frozen with decreasing temperature due to the rather high ionization energy of dopants. The ionization energy of the main donor impurities in 4H-SiC (nitrogen) is 52 meV, the ionization energy of acceptors (aluminum) is 200 meV [1], i.e., the effect of hole freezing in the p -type layers of $p-i-n$ diodes is stronger than in the n -type layers with decreasing temperature. Simple calculations show that the free electron density in n -type layers severalfold decreases at a temperature of 77 K, while the hole density in p -type layers decreases by several orders of magnitude. In this case, the electrical resistance of the emitter p -type layers in $p-i-n$ diodes sharply increases, whereas their injection efficiency which is also controlled by the free hole concentration decreases. Nevertheless, interest in the study of the low-temperature electrical characteristics of $p-i-n$ diodes based on 4H-SiC recently rose since rather efficient low-temperature injection electroluminescence in the terahertz (THz) spectral range was detected in such diodes [2, 3]. The mechanism of the observed THz emission has not been conclusively identified; however, there is reason to believe that it is similar to the THz-photoluminescence mechanism upon the interband optical excitation of semiconductors doped with shallow impurities [4]. The spectra of low-temperature SiC photoluminescence usually contain bands associated with the recombination of photoexcited carriers at donor–acceptor pairs, exciton recombination, band–impurity recombination, and others. The photoluminescence of SiC of various polytypes, caused by the above recombination mechanisms, spans the short-wavelength (green–violet) region of the visible spectral region and the near-ultra-

violet region. It is clear that the initial transfers of excess carriers (electrons and holes) to impurity levels can in principle be accompanied by emission in the THz region (due to transitions between excited impurity states).

It is clear that a similar THz-emission mechanism is also possible during the injection pumping of excess carriers in forward-biased $p-i-n$ diodes based on 4H-SiC.

When the diode operates in the forward direction, the impact ionization of neutral acceptor atoms in an electric field is quite probable, which can promote the partial (or even complete) release of frozen holes. Previously, we measured and analyzed the low-temperature (77 K) current–voltage characteristics of $p^+ - p^- - n^+$ diodes based on 4H-SiC with a lightly doped p^- -type base (the acceptor concentration is $2 \times 10^{15} \text{ cm}^{-3}$) [5]. It turned out that holes in the p^- -type base, completely frozen at a temperature of 77 K, are fully released due to the impact ionization of aluminum atoms under fields of $\sim 10 \text{ kV/cm}$.

In the present work, the dynamic characteristics of 4H-SiC diodes with the $p^+ - n^- - n^+$ -structure are studied (in the pulse mode). To this end, the time dependences of the current are measured when high-amplitude forward-bias pulses are applied to the diode. The work is aimed at studying the impurity-breakdown effect in a heavily doped p^+ -type emitter on the dynamics of an increase in forward current.

2. SAMPLES AND MEASUREMENT TECHNIQUE

Diodes (Fig. 1) were fabricated based on an n^+ -type 4H-SiC wafer with sequentially grown epitaxial n^- and p^+ -type layers (the wafer was purchased on a commercial basis at Cree Inc (USA)). In the studied diodes,

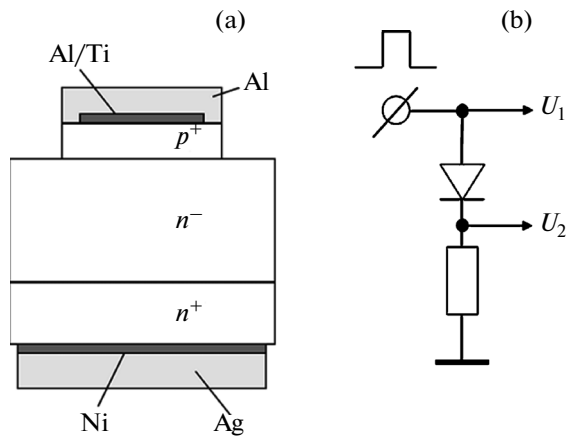


Fig. 1. (a) Cross section of mesa epitaxial $p^+-n^-n^+$ diodes based on $4H$ -SiC. (b) Circuit of pulsed measurements.

the p^+ -type layer is $2\ \mu\text{m}$ thick with an acceptor concentration of $>10^{19}\ \text{cm}^{-3}$; the n^- -type layer is $40\ \mu\text{m}$ thick with a donor concentration of $1 \times 10^{15}\ \text{cm}^{-3}$. The diode area is $4 \times 10^{-2}\ \text{cm}^2$. Fabrication of the diode structure included the following processes conventional for the postgrowth technology of $4H$ -SiC devices: optical photolithography, the deposition of ohmic contacts onto the p^+ -type layer (Al/Ti) and onto the n^+ -type substrate (Ni) by the magnetron sputtering of corresponding targets, contact firing in vacuum at a temperature of 950°C , mesa structure etching in SF_6 plasma using a preliminarily deposited Al layer mask, and plate cutting into individual chips. The diodes were tested in a version without a housing. Low-temperature measurements were performed on the diodes immersed in liquid nitrogen.

Electrical measurements were performed in the pulse mode. Pulses produced by a relaxation generator (with a duration of $1.3\ \mu\text{s}$ and a repetition rate of $1\ \text{Hz}$) were applied to the diode with a series load of $12\ \Omega$ (Fig. 1b). The time dependences of the diode current and voltage were recorded using a Tektronix DPO 4104 multichannel digital oscilloscope.

3. EXPERIMENTAL RESULTS AND DISCUSSION

The results of pulsed measurements are shown in Fig. 2: oscillograms 1 show the input voltage (U_1 in Fig. 1b), oscillograms 2 show the load voltage (U_2 in Fig. 1b). The amplitude of the input voltage pulses was varied in the measurements.

On the axis scale shown in Fig. 2, the diode current appreciably increases when the amplitude of the voltage applied to the diode exceeds $66\ \text{V}$. In this case, the current begins to increase with a time delay with respect to the input-pulse edge. We can see that the time delay is shortened with increasing input-pulse

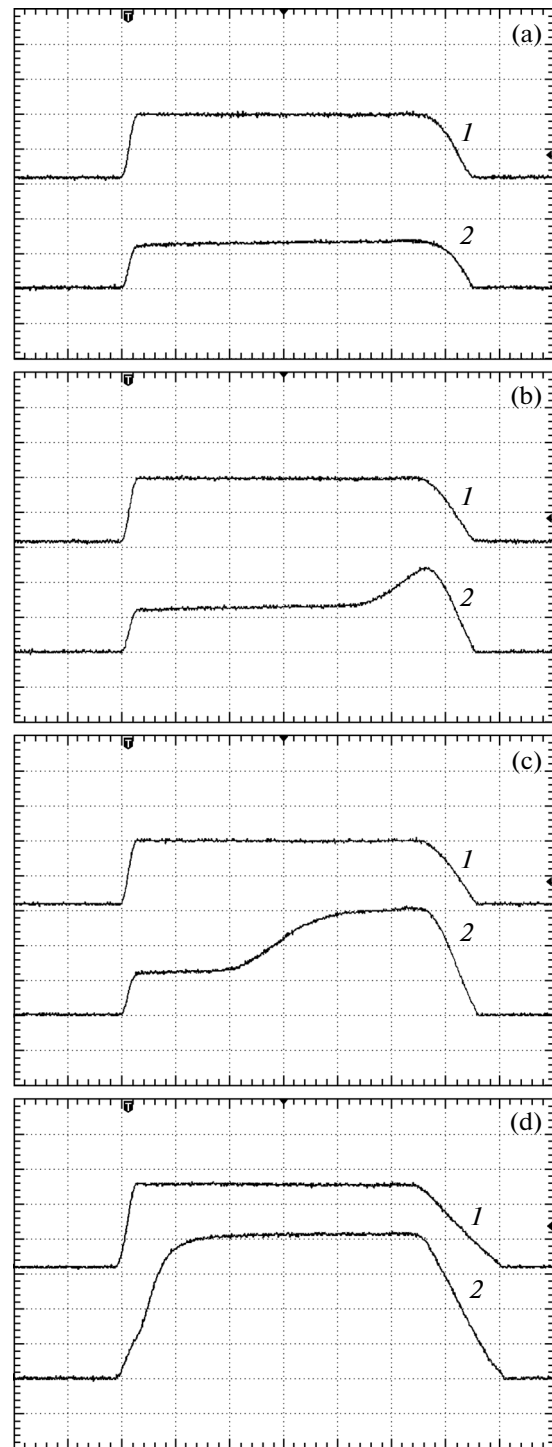


Fig. 2. Oscillograms of voltages (1) U_1 and (2) U_2 after applying voltage pulses of various amplitudes to the diode with an in-series connected load ($12\ \Omega$). The time scale is $200\ \text{ns}/\text{div}$. The voltage scale is (a–c) 50 and (d) $100\ \text{V}/\text{div}$ for U_1 ; (a–c) 20 and (d) $50\ \text{V}/\text{div}$ for U_2 .

amplitude. Simultaneously with a decrease in the delay phase duration, the current-rise phase time decreases and the current amplitude sharply increases.

We note that the diode current oscillograms contain a pedestal, i.e., a rather high initial current flows through the diode.

It is reasonable to believe that the impact ionization of neutral aluminum atoms in p^+ -type regions is responsible for the described processes. At the qualitative level, the time dependences of the current can be described by the simple analytical model presented below, which considers hole generation due to the thermal and impact ionization of neutral acceptor aluminum atoms and free hole retrapping by ionized acceptors.

3.1. Kinetics of Generation–Recombination processes (Analytical Model)

In the case of a single-level model of acceptors, the time (t) dependence of the free hole concentration (p) is described by the equation

$$\frac{dp}{dt} = A_{\text{imp}}(N_A - p)p + A_{\text{th}}(N_A - p) - Bp^2, \quad (1)$$

where N_A is the acceptor concentration, A_{imp} is the acceptor impact-ionization coefficient depending on the field, A_{th} is the thermal-ionization coefficient, and B is the retrapping coefficient. Let us introduce the following notations

$$a = -(A_{\text{imp}} + B), \quad (2)$$

$$b = A_{\text{imp}}N_A - A_{\text{th}}, \quad (3)$$

$$c = A_{\text{th}}N_A. \quad (4)$$

Then Eq. (1) can be rewritten as

$$\frac{dp}{dt} = ap^2 + bp + c. \quad (5)$$

After separating variables, Eq. (5) is easily integrated,

$$\int_{p_0}^p \frac{dp}{ap^2 + bp + c} = \int_0^t dt = t. \quad (6)$$

Here, $p(0) = p_0$, $p(t) = p$.

As follows from formulas (2)–(4), $b^2 - 4ac > 0$. In this case,

$$\int_{p_0}^p \frac{dp}{ap^2 + bp + c} = -\frac{2}{\sqrt{b^2 - 4ac}} \times \left(\operatorname{arctanh} \frac{2ap + b}{\sqrt{b^2 - 4ac}} - \operatorname{arctanh} \frac{2ap_0 + b}{\sqrt{b^2 - 4ac}} \right) = t. \quad (7)$$

Let us introduce the following notation

$$\frac{2}{\sqrt{b^2 - 4ac}} \equiv \tau; \quad ap_0 + \frac{b}{2} \equiv \frac{1}{t_0}. \quad (8)$$

Then expression (7) can be written as

$$\operatorname{arctanh} \left[\tau \left(ap + \frac{b}{2} \right) \right] = -\frac{t}{\tau} + \operatorname{arctanh} \frac{\tau}{t_0}. \quad (9)$$

Then we introduce the following notation

$$\tau \operatorname{arctan} \frac{\tau}{t_0} \equiv t_d, \quad \tau a = -\frac{1}{p^*}. \quad (10)$$

Then the time dependence of the free hole concentration can be written as

$$p = p^* \left(\frac{b\tau}{2} + \tanh \frac{t - t_d}{\tau} \right). \quad (11)$$

The meaning of the last formula becomes most clear if we neglect the thermal-ionization rate and the initial carrier concentration (such an assumption is valid at rather low temperatures). In this case,

$$c = 0, \quad \tau = t_0 = t_d = \frac{2}{b} = \frac{2}{A_{\text{imp}}N_A}, \quad (12)$$

$$p = p_{\text{st}} \left(1 + \tanh \frac{t - \tau}{\tau} \right). \quad (13)$$

In formula (13), $p_{\text{st}} = 2p^*$ is no more than the steady-state value of the free hole concentration at $t \rightarrow \infty$, τ is the characteristic rise time of the hole concentration, and $t_d = \tau$ is the characteristic delay time. The steady-state hole concentration ($p_{\text{st}} \leq N_A$) is defined by the ratio of the impact ionization and retrapping coefficients,

$$p_{\text{st}} = \frac{N_A}{1 + B/A_{\text{imp}}}. \quad (14)$$

At the qualitative level, the above experimental results are described by the model considered above. Indeed, the model predicts the following experimentally observed characteristic features of the dynamics of impurity-breakdown development.

(i) Beginning of a current increase with a time delay which decreases with applied electric field.

(ii) Shortening of the duration of the current rise phase with applied electric field.

(iii) Increase in the steady-state current with applied electric field.

More detailed (quantitative) analysis of the time dependences of the diode current with the purpose of determining the dependences of the impact-ionization coefficients on the electric field is complicated since it is not known with certainty what fraction of the applied external voltage drops at the diode p^+ -type region. At liquid nitrogen temperature, the resistance

of the thin heavily doped p^+ -type layer is rather low (an appreciable initial current flows through the diode); therefore, for the development of impact ionization in the p^+ -type layer, rather large forward bias should be applied to the diode.

4. CONCLUSIONS

Finally, we it can be noted that THz electroluminescence in $4H$ -SiC diodes can potentially occur at temperatures higher than 77 K as well; therefore, studies of the electrical characteristics of diodes in a wide range of lower temperatures remain urgent. Furthermore, studies of the impurity breakdown of acceptors in $4H$ -SiC are also of interest from the viewpoint of the possible development of an inverted population of excited states of impurity atoms and coherent radiation generation.

ACKNOWLEDGMENTS

This study was supported by the Physical Science Branch of the Russian Academy of Sciences (program

“Problems of Radiophysics”, section “Terahertz Range Adoption”).

REFERENCES

1. G. Pensil, F. Ciobanu, T. Fran, M. Krieger, S. Reshanov, F. Schmid, and M. Weidner, *Int. J. High Speed Electron. Syst.* **15**, 705 (2005).
2. Yu. B. Vasil'ev, P. A. Ivanov, A. S. Potapov, T. P. Samsonova, G. Yu. Vasil'eva, Yu. L. Ivanov, A. O. Zakhar'in, V. I. Sankin, A. V. Bobylev, J. Gupta, J. Kolodzey, and A. V. Andrianov, in *Proceedings of the 17th International Symposium on Nanophysics and Nanoelectronics* (Nizh. Novgorod, 2013), vol. 2 (sect. 3), p. 384.
3. A. V. Andrianov, J. P. Gupta, J. Kolodzey, V. I. Sankin, A. O. Zakhar'in, and Yu. B. Vasilyev, *Appl. Phys. Lett.* **103**, 221101 (2013).
4. A. V. Andrianov, A. O. Zakhar'in, Yu. L. Ivanov, and M. S. Kipa, *JETP Lett.* **91**, 96 (2010).
5. I. V. Grekhov, P. A. Ivanov, A. S. Potapov, and T. P. Samsonova, *Semiconductors* **41**, 542 (2007).

Translated by A. Kazantsev